

## Self-reinforcing process of the reconnection electric field in the electron diffusion region and onset of collisionless magnetic reconnection

This article has been downloaded from IOPscience. Please scroll down to see the full text article.

2013 Plasma Phys. Control. Fusion 55 085019

(<http://iopscience.iop.org/0741-3335/55/8/085019>)

View [the table of contents for this issue](#), or go to the [journal homepage](#) for more

Download details:

IP Address: 218.22.21.3

The article was downloaded on 18/06/2013 at 01:53

Please note that [terms and conditions apply](#).

# Self-reinforcing process of the reconnection electric field in the electron diffusion region and onset of collisionless magnetic reconnection

Quanming Lu, San Lu, Can Huang, Mingyu Wu and Shui Wang

Department of Geophysics and Planetary Science, University of Science and Technology of China, Hefei 230026, People's Republic of China

E-mail: [qmlu@ustc.edu.cn](mailto:qmlu@ustc.edu.cn)

Received 28 October 2012, in final form 17 May 2013

Published 17 June 2013

Online at [stacks.iop.org/PPCF/55/085019](http://stacks.iop.org/PPCF/55/085019)

## Abstract

The onset of collisionless magnetic reconnection is considered to be controlled by electron dynamics in the electron diffusion region, where the reconnection electric field is balanced mainly by the off-diagonal electron pressure tensor term. Two-dimensional particle-in-cell simulations are employed in this paper to investigate the self-reinforcing process of the reconnection electric field in the electron diffusion region, which is found to grow exponentially. A theoretical model is proposed to demonstrate such a process in the electron diffusion region. In addition the reconnection electric field in the pileup region, which is balanced mainly by the electromotive force term, is also found to grow exponentially and its growth rate is twice that in the electron diffusion region.

(Some figures may appear in colour only in the online journal)

## 1. Introduction

Magnetic reconnection, known as an effective mechanism for fast energy conversion from magnetic energy to plasma energy, is widely considered to be the primary candidate for many explosive phenomena in solar atmosphere [1–3], the Earth's magnetosphere [4–6], laboratory experiments [7–9] and even the magnetotail of a non-magnetized planet [10–12]. Although it is generally accepted that the nonlinear evolution of collisionless magnetic reconnection and the resulting reconnection rate are dominated by the Hall effect in the ion diffusion region [13–15], the onset of magnetic reconnection is still less understood. From a theoretical point of view, the onset of magnetic reconnection is to explain how reconnection is developed out of the numerical noise in a current sheet [16], which is considered to be controlled by electron dynamics in the electron diffusion region [17–19]. The onset of magnetic reconnection includes two aspects: (1) how an initial reconnection electric field is generated, and (2) how the reconnection electric field grows spontaneously. Several microphysical processes, such as tearing mode [20] or lower

hybrid drift waves [16, 21], have been proposed to provide the initial reconnection electric field, while both simulations and laboratory observations have verified the spontaneous growth of the reconnection electric field [22, 23].

Assuming a two-fluid model for the plasma, the electric field can be obtained directly from the electron momentum equation without further approximation, which is [22, 24]

$$\mathbf{E} = -\mathbf{V}_e \times \mathbf{B} - \frac{\nabla \cdot \bar{\mathbf{P}}_e}{en_e} - \frac{m_e}{e} \frac{d\mathbf{V}_e}{dt}, \quad (1)$$

where  $\mathbf{E}$  and  $\mathbf{B}$  are the electric field and magnetic field, respectively,  $\bar{\mathbf{P}}_e$  is the electron pressure tensor,  $n_e$  and  $\mathbf{V}_e$  are the electron density and bulk velocity, respectively. In a two-dimensional (2D) system ( $\partial/\partial y = 0$ ), the reconnection electric field, which is pointed to the  $y$  direction, can be written in the form [25, 26]

$$E_y = - (V_{ez} B_x - V_{ex} B_z) - \frac{1}{n_e e} \left( \frac{\partial P_{exy}}{\partial x} + \frac{\partial P_{eyz}}{\partial z} \right) - \frac{m_e}{e} \left( \frac{\partial V_{ey}}{\partial t} + V_{ex} \frac{\partial V_{ey}}{\partial x} + V_{ez} \frac{\partial V_{ey}}{\partial z} \right). \quad (2)$$

The first, second and third terms on the right-hand side of equation (2) represent the electromotive force term, the off-diagonal electron pressure tensor term and the electron inertia term, respectively. The presence of the reconnection electric field in the vicinity of the X line implies a violation of the frozen-flux condition, which allows the reconnection process to proceed. In the electron diffusion region, the electrons are demagnetized and not frozen in the magnetic field, and the reconnection electric field is contributed mainly by the off-diagonal electron pressure term [25, 27, 28].

In this paper, first 2D particle-in-cell (PIC) simulations are employed to study the self-reinforcing process of the reconnection electric field in the electric diffusion field during anti-parallel magnetic reconnection, which is balanced mainly by the off-diagonal electron pressure term. Then a theoretical model is proposed to demonstrate such a process.

## 2. Simulation results

A 2D PIC simulation model is used to investigate the self-reinforcing process of the reconnection electric field in the electron diffusion region. In the model, the electromagnetic fields are defined on the grids and updated by solving the Maxwell equations with a full explicit algorithm, and the ions and electrons are advanced in the electromagnetic field. The initial equilibrium configuration is a one-dimensional (1D) Harris current sheet in the  $(x, z)$  plane, where the initial magnetic field and the corresponding number density are given by

$$B_0(z) = B_0 \tanh(z/\delta) e_x, \quad (3)$$

$$n(z) = n_b + n_0 \operatorname{sech}^2(z/\delta), \quad (4)$$

where  $B_0$  is the asymptotic magnitude of the magnetic field,  $\delta$  is the half-width of the current sheet,  $n_b$  is the number density of the background plasma and  $n_0$  is the peak Harris number density. At the same time, the initial distribution functions for the ions and electrons are Maxwellian with drift speed in the  $y$  direction, and the drift speeds satisfy the equation  $V_{i0}/V_{e0} = -T_{i0}/T_{e0}$ , where  $V_{i0}(V_{e0})$  and  $T_{i0}(T_{e0})$  are the initial drift speed and temperature of ions(electrons), respectively. In our simulation, we set  $T_{i0}/T_{e0} = 4$ , and  $n_b = 0.2n_0$ . We set a small initial half-width of the Harris current sheet, which is  $\delta = 0.25c/\omega_{pi}$  (where  $c/\omega_{pi}$  is the ion inertial length defined by  $n_0$ ), therefore, the current sheet is unstable to the tearing instability [20, 29]. The mass ratio  $m_i/m_e$  is chosen to be 64. The light speed is  $c = 15v_A$ , where  $v_A$  is the Alfvén speed based on  $B_0$  and  $n_0$ .

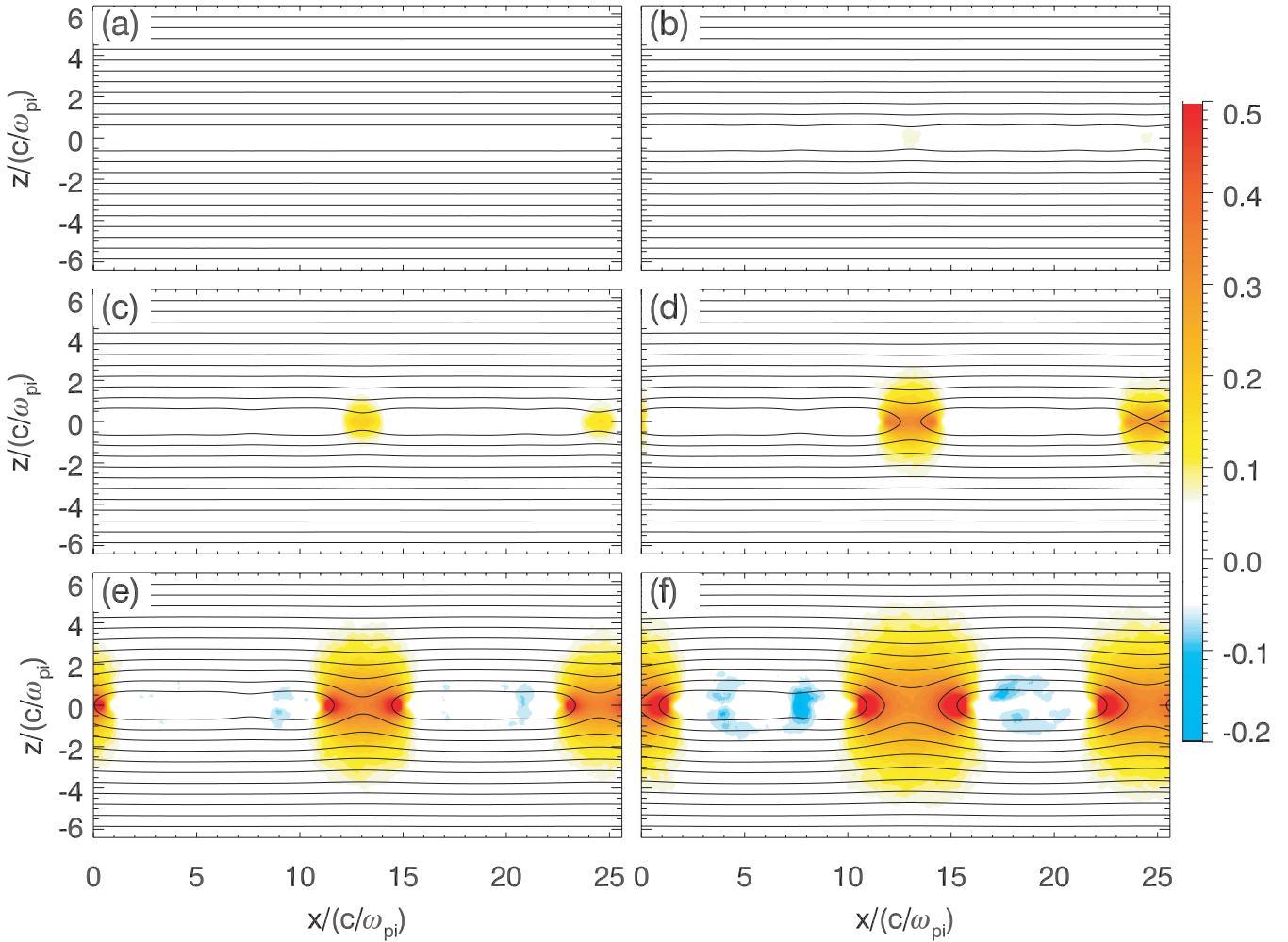
The computation is carried out in a rectangular domain in the  $(x, z)$  plane with the dimension  $L_x \times L_z = (25.6c/\omega_{pi}) \times (12.8c/\omega_{pi})$ . The grid number is  $N_x \times N_z = 1024 \times 512$ . Therefore, the spatial resolution is  $\Delta x = \Delta z = 0.025c/\omega_{pi} = 0.2c/\omega_{pe}$ . The time step is  $\Omega_i t = 0.001$ , where  $\Omega_i = eB_0/m_i$  is the ion gyrofrequency. We employ more than  $10^8$  particles per species to simulate the plasma. The periodic boundary conditions are used along the  $x$  direction; at the same time, ideal conducting boundary conditions for the electromagnetic fields and reflected boundary conditions for particles are used in the  $z$  direction.

Figure 1 shows the reconnection electric field  $(c/v_A)E_y/B_0$  at  $\Omega_i t = (a) 0.5, (b) 10, (c) 11, (d) 12, (e) 13$  and  $(f) 14$ . In the figure, the magnetic field lines are also plotted for reference. At about  $\Omega_i t = 10$ , two obvious X lines begin to be formed around  $x = 12.8$  and  $24.5c/\omega_{pi}$ , respectively. Then, the reconnection electric field around two X lines grows rapidly, and the width of the current sheet also increases. The maximum value of the reconnection electric field is first at the center of the X lines, and finally in the pileup regions around the X lines.

A detailed analysis shows that the process of reconnection has two stages. Figure 2 plots the time evolution of the magnetic flux  $\psi/(B_0c/\omega_{pi})$  along  $z = 0$ . The current sheet is unstable to the tearing mode, which is excited at the first stage. We can find that the most unstable mode is around  $M = 6$  (where  $M = L_x/(2\pi/k_x)$ , and  $k_x$  is the wave number of the tearing modes). Therefore, the most unstable mode satisfies  $k_x\delta \approx 0.37$ . The results are consistent with the linear theory [20, 29]. However, the tearing mode saturates quickly. Therefore, the tearing mode can only provide the initial growth of the reconnection, but it cannot drive the fast reconnection. The second stage begins at about  $\Omega_i t = 10$ ; two X lines are formed at about  $x = 12.8$  and  $24.5c/\omega_{pi}$ , which is a self-reinforcing process.

The growth of the tearing mode and its saturation can also be found in figure 3, which depicts the time evolution of the maximum values of the magnetic flux  $|\psi_M/(B_0c/\omega_{pi})|^2$ , which correspond to modes  $M = 6, 7$  and  $8$ , respectively. The wave numbers are  $k_x\delta \approx 0.37, 0.43$  and  $0.49$ . They grow exponentially. However, they quickly saturate at about  $\Omega_i t = 11$ , when the fast reconnection begins. The linear growth stage of the tearing mode can be demonstrated more clearly in figure 4, which shows the magnetic field lines at  $\Omega_i t = (a) 0.5, (b) 3, (c) 4.5, (d) 5.5$  and  $(e) 6.5$ . Obviously, with the development of the tearing mode, about seven small magnetic islands are formed at the center of the current sheet.

In order to investigate the self-reinforcing process of the fast reconnection, we separate the reconnection electric field into the electromotive force term and the off-diagonal electron pressure tensor term according to equation (2). Compared with the other two terms, the electron inertia term is very small and negligible. Figure 5 shows the reconnection electric field (the left panel), the electromotive force term (the middle panel) and the off-diagonal electron pressure tensor term (the right panel) in the vicinity of the X line, whose center is around  $x \approx 12.8c/\omega_{pi}$ . In the figure,  $(a), (b), (c)$  and  $(d)$  represent the time  $\Omega_i t = 10.0, 10.5, 11.0$  and  $11.5$ , respectively. In the figure, the magnetic field lines are also plotted for reference. The reconnection electric field can be obviously identified in the vicinity of the X line. Consistent with the previous results [22, 27], at the X point the reconnection electric field is balanced mainly by the off-diagonal electron pressure tensor term, while the electromotive force term forms the structure of the reconnection electric field away from the X line with the peaks in the pileup regions. This can be demonstrated more clearly in figure 6, which shows the profile of the reconnection electric field, the electromotive force term and the off-diagonal electron pressure tensor term along  $z = 0$  at  $\Omega_i t = (a) 10.0, (b) 10.5, (c) 11.0$  and  $(d) 11.5$ , respectively. The electromotive



**Figure 1.** Reconnection electric field  $(c/v_A)E_y/B_0$  at  $\Omega_i t = (a) 0.5, (b) 10, (c) 11, (d) 12, (e) 13$  and  $(f) 14$ . In the figure, the magnetic field lines are also plotted for reference.

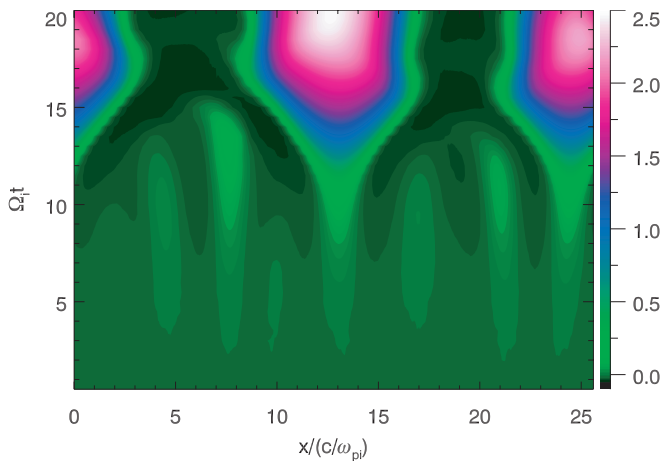


**Figure 2.** Time evolution of the magnetic flux  $\psi/(B_0 c/\omega_{pi})$  along the line  $z = 0$ .

force term supports the reconnection electric field at  $|x - L_X| \geq 0.3c/\omega_{pi}$ , where  $L_X$  is the position of the X line. At the same time, the amplitude of both the off-diagonal electron pressure tensor and the electromotive force terms increase with time. The growth rate of the electromotive force term is much larger

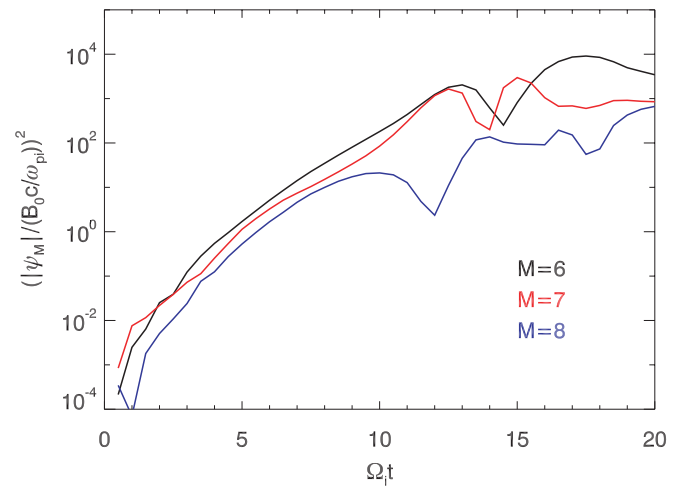


**Figure 3.** Time evolution of the maximum values of the magnetic flux  $|\psi_M/(B_0 c/\omega_{pi})|^2$ , which correspond to modes  $M = 6, 7$  and  $8$ , respectively.

than that of the off-diagonal electron pressure tensor term. Such a self-reinforcing process of the reconnection electric field can be described more clearly in figure 7. In the figure, the red line shows the time evolution of the maximum amplitude

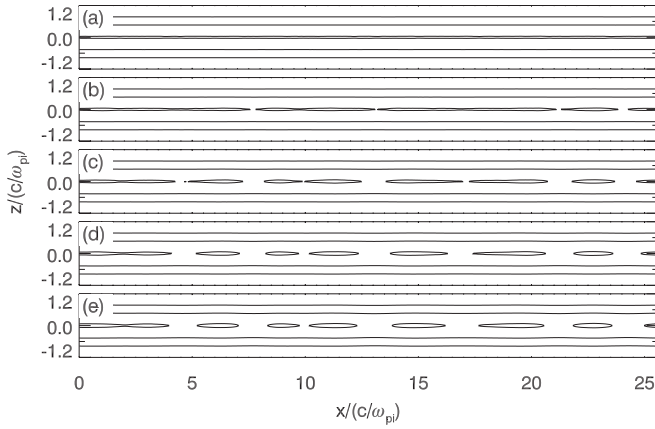


**Figure 4.** Magnetic field lines at  $\Omega_i t = (a) 0.5, (b) 3, (c) 4.5, (d) 5.5, (e) 6.5$  during the linear growth stage of the tearing mode.

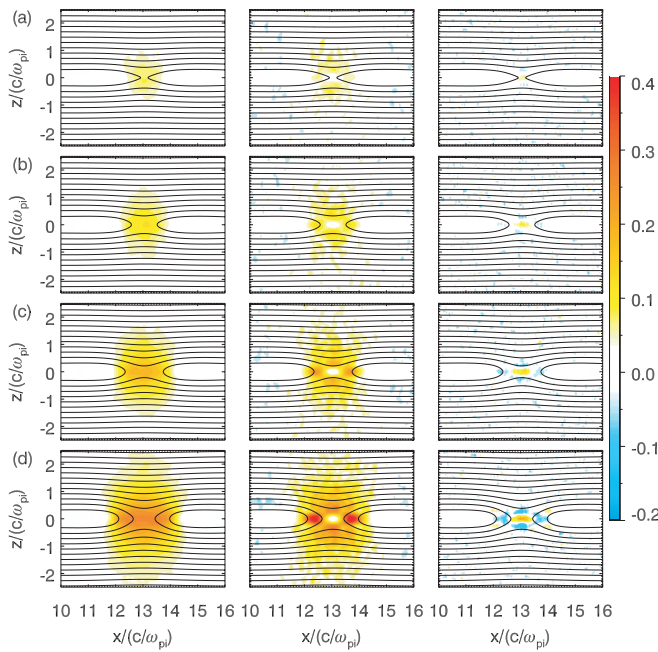


**Figure 5.** Reconnection electric field (the left panel), the electromotive force term (the middle panel) and the off-diagonal electron pressure tensor term (the right panel) in the vicinity of the X line, whose center is around  $x \approx 12.8c/\omega_{pi}$ . (a), (b), (c) and (d) represent the time  $\Omega_i t = 10.0, 10.5, 11.0$  and  $11.5$ , respectively. In the figure, the magnetic field lines are also plotted for reference.

of the off-diagonal electron pressure tensor term along the line  $z = 0$ , while the black line describes the time evolution of the maximum amplitude of the electromotive force term along the line  $z = 0$ . The growth rates of the electromotive force term and the off-diagonal electron pressure tensor term during the self-reinforcing process of the reconnection are also shown in the figure, which are calculated to be about 0.50 and 0.29, respectively. We can also find that the growth of both the electromotive force term and the off-diagonal electron pressure tensor term stop at about  $\Omega_i t = 12.0$ .

### 3. Theoretical model

The self-reinforcing process of the off-diagonal electron pressure tensor terms in the 2D PIC simulations can be

demonstrated with a theoretical analysis. The ion diffusion region can be divided into two parts: an ion-scale outer region and an electron-scale inner region, as shown in figure 8. The scale of the inner electron diffusion region is determined by the trapping length of electrons in a field reversal, where electrons are unmagnetized. After analyzing electron orbits in field reversals, Biskamp and Schindler [28] found that the lengths in the  $x$  and  $z$  directions can be expressed as

$$\lambda_x = \left[ \frac{2m_e T_e}{e^2 \left( \frac{\partial B_z}{\partial x} \right)^2} \right]^{1/4}, \quad \lambda_z = \left[ \frac{2m_e T_e}{e^2 \left( \frac{\partial B_z}{\partial z} \right)^2} \right]^{1/4}, \quad (5)$$

where  $T_e$  is the electron temperature, and  $x$  direction refers to the outflow direction. Similar results were also obtained by Kuznetsova *et al* [30]. In the electron diffusion region, the reconnection electric field is balanced mainly by the off-diagonal electron pressure tensor term, which can be given as [31]

$$E_{yO} \approx \frac{1}{e} \frac{\partial V_{ex}}{\partial x} \sqrt{2m_e T_e}, \quad (6)$$

where  $V_{ex}$  is the electron bulk velocity in the  $x$  direction. The validity of equation (6) is demonstrated in figure 9, which plots the evolution of the reconnection electric field obtained from the simulations. The black line shows the reconnection electric field, which is obtained directly from the simulations. The red line exhibits the reconnection electric field, which is calculated using the following method: first we obtain the electron bulk velocity  $V_{ex}$  and temperature  $T_e$  from the simulations, and then the reconnection electric field is calculated using equation (6).

During the self-reinforcing process of the reconnection electric field (from about  $\Omega_i t = 10$  to  $\Omega_i t = 12$ ), as shown in this paper, the sizes of the electron diffusion region ( $\lambda_x$  and  $\lambda_z$ ) change little, and the electrons are hardly thermalized in the electron diffusion region. Therefore, we can assume that the sizes of the electron diffusion region are fixed and the electron temperature is kept as a constant. Then

$$E_{yO} \approx \frac{V_{ex,M} \sqrt{2m_e T_e}}{e \lambda_x}, \quad (7)$$

where  $V_{ex,M}$  is the electron bulk velocity just outside of the electron diffusion region.

At the same time, the electrons are unmagnetized in the electron diffusion region, the reconnection electric field  $E_{yO}$  is determined by the off-diagonal electron pressure tensor term. However, it is generally accepted that the electron bulk velocity in the electron diffusion region is decided by the electric field, while the existence of the magnetic field leads to the off-diagonal electron pressure tensor term, which is approximately equal to the reconnection electric field in the electron diffusion region. If the electrons have sufficiently large energy and their gyroradii are much larger than the curvature radius of the magnetic field, these electrons are unmagnetized and their motions are governed by  $m_e \frac{dv_e}{dt} = -eE$ . Therefore, the electron bulk velocity in the  $y$  direction is proportional to the reconnection electric field, which can be expressed as [32]

$$\frac{dV_{ey}}{dt} \propto E_{yO}. \quad (8)$$

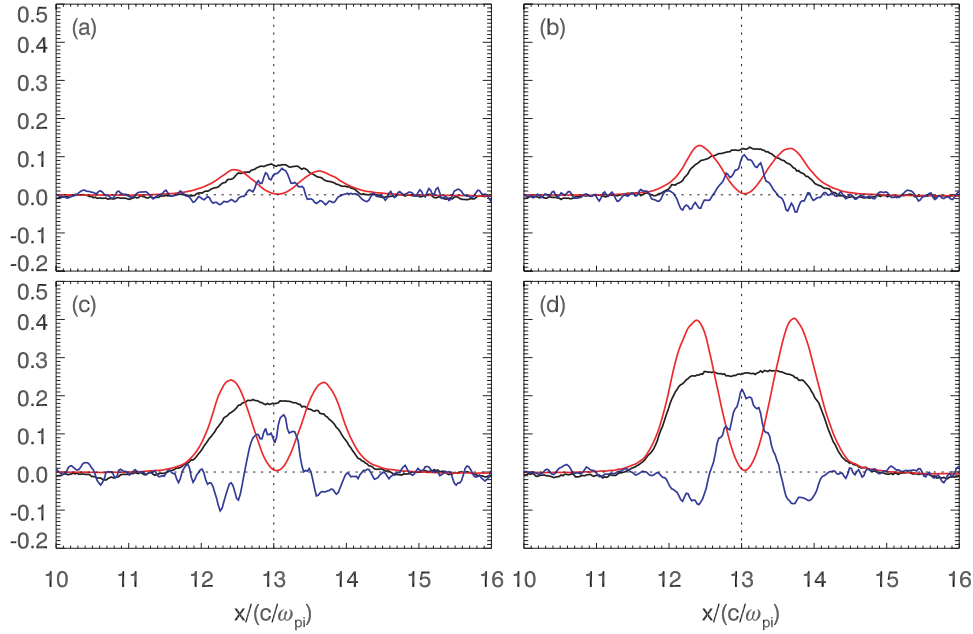


**Figure 6.** Profile of the reconnection electric field (the black lines), the electromotive force term (the red lines) and the off-diagonal electron pressure tensor term (the blue lines) along  $z = 0$  at  $\Omega_i t = (a) 10.0, (b) 10.5, (c) 11.0$  and  $(d) 11.5$ .

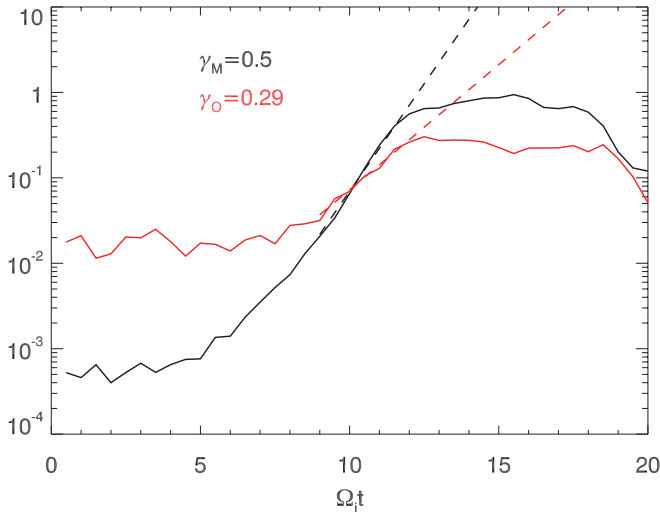


**Figure 7.** Time evolution of the maximum amplitudes of the electromotive force term and the off-diagonal electron pressure tensor terms along the line  $z = 0$ , which are denoted by the black and red solid lines, respectively. The growth rates of the electromotive force term and the off-diagonal electron pressure tensor terms during the self-reinforcing process are also shown in the figure, which are represented by the black and red dashed lines, respectively.

As the electrons leave the electron diffusion region and become magnetized again, the gyromotion transfers their velocity from the  $y$  direction to the  $x$  and  $z$  directions [33]. Therefore, on average  $V_{ex,M}$  and  $V_{ez,M}$  (where  $V_{ez,M}$  is the electron bulk velocity in the  $z$  direction just outside the electron diffusion region) outside of the electron diffusion region are proportional to  $V_{ey}$  inside the electron diffusion region. Then,

$$\frac{dV_{ex,M}}{dt} \propto \frac{dV_{ey}}{dt} \propto E_{y0}. \quad (9)$$

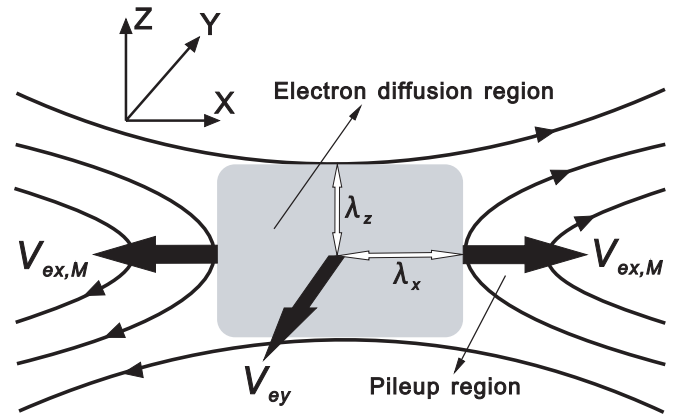


**Figure 8.** Schematic for the generation of the electromotive force term and the off-diagonal electron pressure tensor terms.

Then, we can obtain

$$\frac{dV_{ex,M}}{dt} \propto \frac{v_{the}}{\lambda_x} V_{ex,M}, \quad (10)$$

where  $v_{the} = \sqrt{2T_e/m_e}$  is the electron thermal velocity. Therefore, the off-diagonal electron pressure tensor term in the electron diffusion region  $E_{y0}$  and the electron bulk velocity  $V_{ex,M}$  grow exponentially, with  $E_{y0} \propto e^{\gamma_O t}$ . The growth rate  $\gamma_O \propto v_{the}/\lambda_x$ . The existence of the reconnection electric field can accelerate the electrons in the electron diffusion region, and the electrons obtain a bulk velocity just outside the electron diffusion region, which can in turn make  $E_{y0}$  larger.

Now let us focus on the electromotive force term of the reconnection electric field away from the X line. In a 2D system ( $\partial/\partial y = 0$ ), we can get  $\partial B_z/\partial t = -\partial E_y/\partial x$ , according to  $\partial \mathbf{B}/\partial t = -\nabla \times \mathbf{E}$ . Through an integral circling the pileup region, after the size of the pileup region is assumed to be fixed, it is easy to obtain  $\partial B_z/\partial t \propto E_{y0}$ . Then  $B_z \propto e^{\gamma_O t}$ .

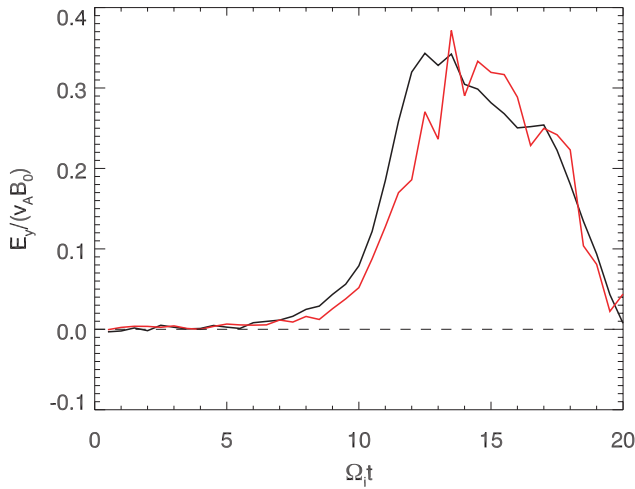


**Figure 9.** Evolution of the reconnection electric field obtained from the simulations. The black line shows the reconnection electric field, which is obtained directly from the simulations. The red line exhibits the reconnection electric field, which is calculated using equation (6).

The physical mechanism of the growth of  $B_z$  can be described as follows: the electrons get a bulk velocity after they are accelerated in the electron diffusion region. The magnetic field is then brought out of the electron diffusion region and piled up just outside of the electron diffusion region, which make the magnetic field grow exponentially.

Therefore, in the pileup region, the reconnection electric field is balanced mainly by the electromotive force term, which can be expressed as

$$E_{yM} = -V_{ex,M} B_z \propto e^{2\gamma_0 t}. \quad (11)$$

However, with the accumulation of the magnetic field in the pileup region, the increase in the electron outflow speed will stop. Then the growth of the reconnection electric field saturates, and a nearly steady state is attained, as shown in figure 6 after about  $\Omega_1 t = 12.0$ .

The theoretical model also predicts that the growth rate of the reconnection electric field is proportional to the square root of the initial electron temperature. In order to test this prediction, we perform an additional 2D PIC simulation run with the electron temperature half of the original value, while the other parameters are kept the same. The structure of the reconnection is almost the same (not shown); as predicted, the growth rate of the reconnection electric field decreases. Figure 10 shows the self-reinforcing process of the reconnection electric field. In the figure, the red line shows the time evolution of the maximum amplitude of the off-diagonal electron pressure tensor term along the line  $z = 0$ , while the black line describes the time evolution of the maximum amplitude of the electromotive force term along the line  $z = 0$ . The growth rates of the electromotive force term and the off-diagonal electron pressure tensor term during the self-reinforcing process of the reconnection are also shown in the figure, which are calculated to be about 0.42 and 0.22, respectively. The results are consistent with the theoretical prediction, and the difference may come from the assumptions used in our theoretical model, such as the fixed electron temperature.

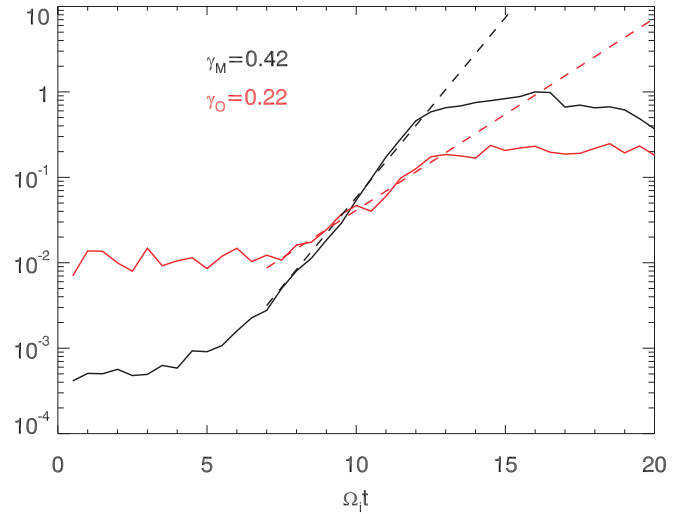


**Figure 10.** Time evolution of the maximum amplitudes of the electromotive force term and the off-diagonal electron pressure tensor terms along the line  $z = 0$ , which are denoted by the black and red solid lines, respectively. Here, the initial electron temperature is half of the original case. The growth rates of the electromotive force term and the off-diagonal electron pressure tensor terms during the self-reinforcing process are also shown in the figure, which are represented by the black and red dashed lines, respectively.

#### 4. Conclusions and discussion

In this paper, first we employ 2D PIC simulations to investigate the self-reinforcing of the reconnection electric field in anti-parallel magnetic reconnection. The process of reconnection has two stages: the tearing mode is excited at the first stage, and it saturates quickly, and then the self-reinforcing process of the reconnection electric field occurs. During the self-reinforcing of the reconnection, the reconnection electric field in the electron diffusion regions is balanced mainly by the off-diagonal electron pressure tensor term, while the reconnection electric field in the pileup regions is supported mainly by the electromotive force term. The reconnection electric fields in both the electron diffusion region and the pileup regions grow exponentially, and the growth rate in the pileup region is 1.7–1.9 times that in the electron diffusion region. Then, we propose a theoretical model to explain the self-reinforcing process of the reconnection electric field in the electron diffusion region. The self-reinforcing process of the off-diagonal electron pressure tensor term can be described as follows: the existence of the reconnection electric field can accelerate the electrons in the electron diffusion region, and the electrons obtain a bulk velocity; the gradient of the electron bulk velocity can in turn support the off-diagonal electron pressure tensor term of the reconnection electric field, which make both the electron bulk velocity and the off-diagonal electron pressure tensor term grow exponentially. In the region away from the X line, the reconnection electric field is balanced mainly by the electromotive force term. After the electrons are accelerated in the electron diffusion region, they get a bulk velocity. Then, the magnetic field is brought out of the electron diffusion region, and it is piled up just outside of the electron diffusion region, which make the magnetic field grow

exponentially in this region. Therefore, the electromotive force term in this region grows much faster (about twice) than the off-diagonal electron pressure tensor term in the electron diffusion region, which is consistent with the simulation results. The difference comes from the assumptions used in our theoretical work, such as the fixed size of the electron diffusion region and constant electron temperature.

In this paper, we concentrate on the initial growth stage of magnetic reconnection, and ion dynamics is not important during this process. A larger system should be used if the effects of ion dynamics on the reconnection are considered. During the self-reinforcing process of the reconnection electric field, the magnetic field is accumulated in the pileup region, which will decelerate the electron outflow until the increase in the electron outflow speed stops, and then the growth of the reconnection electric field will also end and a nearly steady state may be attained. The current sheet may also be extended later, where secondary islands will be formed, and then the growth rate of the reconnection electric field may also be changed [34–36]. Also in this paper, we do not consider the effects of a guide field, and a guide field will change the electron trajectories and then distort the symmetry of the electron diffusion region [33, 37]. This may change the growth rate of the reconnection electric field in the electron diffusion region.

In addition, in this paper we employ a 2D system, and the tearing modes are assumed to provide the initial reconnection electric field. However, in order to make the tearing modes unstable in the Harris current sheet, a small width is used. In this way, the reconnection electric field will grow much faster and saturate much earlier during its self-reinforcing process than in reality.

## Acknowledgments

This research was supported by the National Science Foundation of China, Grant Nos 41274144, 41174124, 11220101002, 41121003, 41128004, the 973 Program (2012CB825602, 2013CBA01503), the Project of CAS KZZD-EW-01, the Ocean Public Welfare Scientific Research Project and the State Oceanic Administration, People's Republic of China (No 201005017).

## References

- [1] Giovanelli R G 1946 *Nature* **158** 81  
 [2] Masuda S, Kosugi T, Hara H and Ogawara Y 1994 *Nature* **371** 495  
 [3] Song H Q, Chen Y, Li G, Kong X L and Feng S W 2012 *Phys. Rev. X* **2** 021015  
 [4] Baker D N, Pulkkinen T I, Angelopoulos V, Baumjohann W and McPherron R L 1996 *J. Geophys. Res.* **101** 12975  
 [5] Nagai T *et al* 1998 *J. Geophys. Res.* **103** 4419  
 [6] Angelopoulos V *et al* 2008 *Science* **321** 931  
 [7] Wesson J 1997 *Tokamaks* (New York: Oxford University Press)  
 [8] Ji H T, Yamada M, Hsu S and Kulsrud R 1998 *Phys. Rev. Lett.* **80** 3256  
 [9] Li C K *et al* 2007 *Phys. Rev. Lett.* **99** 055001  
 [10] Dong Q L *et al* 2012 *Phys. Rev. Lett.* **108** 215001  
 [11] Eastwood J P *et al* 2008 *Geophys. Res. Lett.* **35** L02106  
 [12] Zhang T L *et al* 2012 *Science* **336** 567  
 [13] Sonnerup B U Ö 1979 Magnetic field reconnection *Solar System Plasma Physics* vol 3 ed L J Lanzèerotti *et al* (New York: North-Holland) p 46  
 [14] Shay M A, Drake J F, Rogers B N and Denton R E 2001 *J. Geophys. Res.* **106** 3759  
 [15] Birn J *et al* 2001 *J. Geophys. Res.* **106** 3715  
 [16] Scholer M, Sidorenko I, Jaroschek C H, Treumann R A and Zeoler A 2003 *Phys. Plasmas* **10** 3521  
 [17] Vasyliunas V M 1975 *Rev. Geophys.* **13** 303  
 [18] Karmabadi H, Daughton W and Scudder J 2007 *Geophys. Res. Lett.* **34** L13104  
 [19] Fujimoto K and Sydora R D 2009 *Phys. Plasmas* **16** 112309  
 [20] Karimabadi H, Daughton W and Quest K B 2004 *Geophys. Res. Lett.* **31** L18801  
 [21] Daughton W 2003 *Phys. Plasmas* **10** 3103  
 [22] Pritchett P L 2001 *J. Geophys. Res.* **106** 3798  
 [23] Egedal J, Fox W, Katz N, Porkolad M, Reim K and Zhang E 2007 *Phys. Rev. Lett.* **98** 015003  
 [24] Cai H J and Lee L C 1997 *Phys. Plasmas* **4** 509  
 [25] Lu Q M, Wang R S, Xie J L, Huang C, Lu S and Wang S 2011 *Chin. Sci. Bull.* **56** 1174  
 [26] Hesse M and Winske D 1998 *J. Geophys. Res.* **103** 26479  
 [27] Yin L and Winske D 2002 *J. Geophys. Res.* **107** 1485  
 [28] Biskamp D and Schindler K 1971 *Plasma Phys.* **13** 1013  
 [29] Coroniti F V 1977 *Phys. Rev. Lett.* **38** 23  
 [30] Kuznetsova M, Hesse M and Winske D 1998 *J. Geophys. Res.* **103** 199  
 [31] Hesse M, Schindler K, Birn J and Kuznetsova M 1999 *Phys. Plasmas* **6** 1781  
 [32] Divin A, Lapenta G, Markidis S, Semenov V S, Erkaev N V, Korovinskiy D B and Biernat H K 2012 *J. Geophys. Res.* **117** A06217  
 [33] Fu X R, Lu Q M and Wang S 2006 *Phys. Plasmas* **13** 012309  
 [34] Daughton W and Scudder J 2006 *Phys. Plasmas* **13** 072101  
 [35] Karmabadi H, Daughton W and Scudder J 2007 *Geophys. Res. Lett.* **34** L13104  
 [36] Wang R S, Lu Q M, Du A M and Wang S 2010 *Phys. Rev. Lett.* **104** 175003  
 [37] Drake J F, Swisdak M, Schoeffler K M, Roger B N and Kobayashi S 2006 *Geophys. Res. Lett.* **33** L13105